Ultraviolet Synchrotron Orbital Radiation Facility

VIII-U Development of the UVSOR Light Source

VIII-U-1 Development of Lattice Components for UVSOR Upgrade Project

KATOH, Masahiro; HAYASHI, Kenji; HONDA, Toru[1]; HORI, Yoichiro[2]; HOSAKA, Masahito; KINOSHITA, Toshio; KODA, Shigeru[3]; TAKASHIMA, Yoshifumi; YAMAZAKI, Jun-ichiro; KITAMURA, Hideo[4]; HARA, Toru[4]; TANAKA, Takashi[4]
([1]KEK-PF; [2]IMS and KEK-PF; [3]Saga Univ.; [4]RIKEN)

We have been developing the lattice components for the UVSOR upgrade project. In this project, the original DBA lattice of the storage ring will be modified to have lower emittance and more straight sections available for insertion devices. The reconstruction will be started in March 2003 and be completed until the end of May. All the quadrupole and sextupole magnets will be replaced with combined function multi-pole magnets, which is capable of producing both quadrupole field and sextupole field. We constructed a prototype and measured the magnetic field. The results have shown that the required field strength and field quality was well realized. We have completed the design of the vacuum system. Their fabrication will be started in September 2002 and be completed until the end of February.

VIII-U-2 Storage Ring Free Electron Laser

HOSAKA, Masahito; KATOH, Masahiro; HAYASHI, Kenji; KINOSHITA, Toshio; KODA, Shigeru[1]; TAKASHIMA, Yoshifumi; YAMAZAKI, Jun-ichiro
([1]Saga Univ.)

At the UVSOR, performance of the free electron lasers has been improved aiming users applications. The average output power has reached 1W level, which is the world highest record as a storage ring free electron laser (SRFEL). SRFEL have a potentiality for scientific applications as a unique light source because of variable wavelength, good coherence, temporal structure, and perfect synchronization with synchrotron radiation (SR). We started an experiment using SRFEL combined with SR. We have succeeded to observe the double-resonant excitation of Xe by using SR and SRFEL as pump and probe lights, respectively.

VIII-U-3 Ion Trapping at UVSOR

MOCHIHASHI, Akira; KATOH, Masahiro; HAYASHI, Kenji; KINOSHITA, Toshio; HOSAKA, Masahito; TAKASHIMA, Yoshifumi; YAMAZAKI, Jun-ichiro

An ion-related vertical instability of the UVSOR electron storage ring was observed in a multi-bunch mode with empty buckets (a bunch gap). In contrast to a shorter bunch train, it was clearly seen that vertical betatron tune had step-like changes with decrease of a beam current in a longer train. The step-like change in the tune seems to be caused by sudden change in condition of stability of trapped ions. Change in amplitude of the vertical betatron oscillation along a bunch train was also observed with a bunch-by-bunch beam diagnostic system. The structure of the amplitude seems to have relation to modulation of the ion density along the train.

VIII-U-4 Design Study of Vacuum System Improvement

HORI, Yoichiro; YAMAZAKI, Jun-ichiro; KATOH, Masahiro; HAYASHI, Kenji; HOSAKA, Masahito; KINOSHITA, Toshio; MOCHIHASHI, Akira

In the UVSOR upgrade project, vacuum beam chambers in straight sections must be replaced to new ones designed for new magnets and their arrangement, and three bending chambers need to be renewed for re-equipment of beam-lines. In the remodeling, the pumping speed distribution should be considered in order to maintain a long beam lifetime in the upgraded ring. The pump arrangement by which a required operating pressure can be achieved was searched by a simple simulation of the pressure distribution. The simulation suggests that the pump location is essential in the straight section, and that the lifetime can be expected to extend up to 10–30 % by reinforcing the pumping speed in every bend section. Also a thermal/structural analysis of the chamber has been carried out for the 500 mA storage. Though the present concept of the stainless steel with partially water-cooling will be inherited, the use of copper material is locally desirable for the parts suffered intense SR. New chambers have been designed in detail with applying above results.

VIII-V Researches by the USE of UVSOR

VIII-V-1 Non-Radiative Decay of the Core Excitons in Auger-Free Luminescence Materials, CsCl and BaF_2

KAMADA, Masao; ITOH, Minoru[1]
([1]Shinshu Univ.)

[*Phys. Rev. B* **65**, 245104 in press]

The present work has been conducted to understand the decay processes of the Cs-5*p* and Ba-5*p* core excitons in CsCl and BaF_2, respectively, where the Auger decay process of the Cs-5*p* and Ba-5*p* core holes is energetically forbidden. The core-exciton peaks are missing in the excitation spectra for the Auger-free luminescence, which arises from a radiative decay of the valence electrons into these core holes. Resonant enhancement effects of the valence-band photoelectron spectra are observed around 13 eV for CsCl and 17 eV for BaF_2. The effects are attributed to the non-radiative decay through the direct-recombination process of an excited electron and the Cs-5*p* or Ba-5*p* core hole forming the core exciton. It is also found that the core exciton deforms its surrounding lattice with relaxation energy of about 0.3 eV in CsCl and 0.9 eV in BaF_2. The non-radiative direct-recombination probabilities of the core excitons are estimated to be about 32 and 75% for CsCl and BaF_2, respectively, by taking account of the lattice relaxation effects.

VIII-V-2 Photoelectron Spectroscopic Study on Photo-Induced Phase Transition of Spin-Crossover Complex

KAMADA, Masao; TAKAHASHI, Kazutoshi; DOI, Yo-ichiro[1]; FUKUI, Kazutoshi[1]; TAYAGAKI, Takeshi[2]; TANAKA, Ko-ichiro[2]
([1]Fukui Univ.; [2]Kyoto Univ.)

[*Phase transition* **41-47**, in press]

Valence band structures in various phases of an organometal spin-crossover complex $[Fe(2\text{-pic})_3]Cl_2 \cdot EtOH$ have been measured by means of photoelectron spectroscopy based on the combination of synchrotron radiation and laser light. The valence band structure showed the remarkable change due to the photo-induced phase transition at low temperatures as well as the thermally induced phase transition, but the structure of the photo-induced phase was very different from that of the high-temperature phase. The DV-Xα calculation based on the FeN_6 cluster was in good agreement with the photoelectron spectra. The present results indicate that the electronic structures originating from Fe and N ions are closely related to the photo-induced phase transition.

VIII-V-3 Surface-Photovoltage Effect in GaAs-GaAsP Super-Lattice Studied with Combination of Synchrotron Radiation and the Laser

TANAKA, Senku[1]; MORÉ, Sam D.; TAKAHASHI, Kazutoshi; KAMADA, Masao; NISHITANI, Tomohiro[2]; NAKANISHI, Tsutomu[2]
([1]GUAS; [2]Nagoya Univ.)

[*SPIN2000* 1000 (2001)]

Core-level photoelectron spectroscopy with the combination of synchrotron radiation (SR) and a laser was used for exploring the surface-photovoltage (SPV) effect and its temporal profiles in a GaAs/GaAsP superlattice (SL). It was observed that the SPV value in the SL is suppressed as compared with a bulk GaAs. However, no significant difference was found in the temporal profile between the bulk and the SL. It is suggested that the suppression of the SPV in the SL is dominantly due to the small value of band bending under thermal equilibrium.

VIII-V-4 Pump/Probe Experiments with FEL and SR Pulses at UVSOR

GEJO, Tatsuo; SHIGEMASA, Eiji; NAKAMURA, Eiken; HOSAKA, Masahito; MOCHIHASHI, Akira; KATOH, Masahiro; YAMAZAKI, Jun-ichiro; HAYASHI, Kenji; TAKASHIMA, Yoshifumi; HAMA, Hiroyuki[1]
([1]Tohoku Univ.)

Synchrotron radiation free electron lasers (SRFEL or FEL) has been used as a light source because of high power, high coherence and its unique temporal feature. Pump and probe experiments using FEL and synchrotron radiation (SR) pulses have been tried to perform for the last decade. This is due to the fact that the FEL pulse naturally synchronizes with the SR pulse. As the first gas-phase experiment combined FEL with SR, we have carried out the two-photon double-resonant excitation on Xe atoms, utilizing a SR pulse as a pump and an FEL pulse as a probe light.

The experiments were performed on BL7B at UVSOR, where a 3-m normal incidence monochromator is installed. The monochromatized SR from a bending magnet was used as the pump light. The estimated photon flux at BL3A1 is about 1×10^{13} photons/sec/-0.1%B.W./100 mA, whereas that at BL7B is in the order of 10^9. The FEL pulses were extracted through the backward mirror, and transported to the experimental station through a series of multi-layer mirrors. The flight path of FEL, which was adjusted to synchronize the timing between the FEL and the SR pulses, was about 30 m. Fine-tuning of the delay timing was made by using a movable optical delay system (50 cm) at the experimental station. The FEL and SR pulses introduced, coaxially crossed an effusive jet of Xe atoms from a gas nozzle. The singly charged Xe ions produced in the interaction region were detected by means of a conventional channeltron.

The first experiment on the two-photon double-resonant excitation of the Xe* $5p^5nf$ autoionization states using the combination of a mode-locked laser [1]

and SR has already been successfully demonstrated by Meyer's group at LURE. The wavelength of SR was adjusted to be 10.4 eV, in order to prepare the Xe* $5p^5 5d$ intermediate states in a first step. The Xe* $5p^5 4f$ autoionization resonance can be excited within the wavelength region of FEL in a second step. Since the lifetime of the intermediate states is quite short (600 ps), the synchronization between the SR and laser pulses is essential in this experiment. The count rate for this measurement is about 200 counts/sec, which is about 1/1000 in comparison to the case when the non-monochromatized undulator radiation was used at BL3A1. Although the photon intensity of SR at BL7B is high enough to obtain total ion yield spectrum, it is found that considerable improvement on the experimental setup is required for measuring the angular distribution of photoelectrons from the same system on this beamline.

We are planning to carry out similar experiments in the shorter wavelength region (around 400 nm) of FEL, where higher Rydberg series of the Xe* $5p^5 nf$ states *via* the Xe* $5p^5 5d$ intermediate state are accessible.

Reference

1) M. Gisselbrecht, A. Marquette and M. Meyer, *J. Phys. B* **31**, L977 (1998).

VIII-V-5 Angle-Resolved Photoion Spectra of SO_2

GEJO, Tatsuo; SHIGEMASA, Eiji; NAGASONO, Mitsuru; OJI, Hiroshi; HATSUI, Takaki; KOSUGI, Nobuhiro

The SO_2 molecule has three unoccupied valence orbitals, $3b_1$*, $9a_1$* and $6b_2$*, which can be associated with the three S 3*p* orbitals, where SO_2 has an electronic structure of $S^{4+}[(3s)^2(3p)^0]\cdot(O^{2-})_2$ in the limit of an ionic bonding picture and the $3b_1$, $9a_1$ and $6b_2$ orbitals correspond to out-of-plane S3*p* π (π_{out}), in-plane S3*p* π (π_{in}) and in-plane S3*p* σ, respectively.[1)] All the S1*s* ($1a_1$) excitations to the $3b_1$*, $9a_1$* and $6b_2$* orbitals are dipole-allowed and are found to be lying below the S1*s* → Rydberg excitations with the term values of 10.4, 5.7, and 4.8 eV, respectively.[1)] The chemical bond between S and O is not so strong, and even the excitation to the most antibonding σ* ($6b_2$) orbital is located below the ionization threshold. The single excitations to all the unoccupied valence orbitals are observed below the ionization threshold even in the case of the O1*s* absorption spectra assigned previously, though there are two O 1*s* orbitals, $1b_2$ and $2a_1$. The $1b_2$–$2a_1$ splitting caused by the interaction between the two O 1*s* orbitals is expected to be negligible and does not change the situation.

The photoabsorption and angle resolved photoion spectra of SO_2, were measured in the O *K*-edge region. The O 1*s* core-to-valence excited states of SO_2 were calculated by multi-reference configuration interaction including single and double excitations (MR-SDCI).

Figure 1a and 1b show the O *K*-edge photoabsorption and angle resolved photoion spectrum of SO_2. The lowest photoabsorption feature A observed at 530.56 eV is well separated from the higher features. The feature A is attributed to the O $1s\sigma(2a_1) \rightarrow \pi^*(3b_1)$ transition, considering its term value of 9.27 eV. It should be noted that the B_1 state is a dipole-allowed out-of-molecular plane (π*) transition from the A_1 ground state, the A_1 and B_2 states are dipole-allowed in-plane transitions, and the A_2 state is dipole-forbidden; the $\pi^*(3b_1)$ orbital is not accessible from the O $1s\sigma$ ($1b_2$) electron. Between the lowest $1s \rightarrow \pi^*$ excitation at 530.56 eV and the O *K*-shell ionization threshold at 539.83 eV, the spectral feature is dominated by some broad bands labeled as B, C, and D at ~ 535 eV (term values of ~ 5 eV) arising from the 1*s* → in-plane excitations, which consist of the O $1s \rightarrow 9a_1$* (dipole-allowed B_2 from $1b_2$ and A_1 from $2a_1$) and O $1s \rightarrow 6b_2$* (dipole-allowed A_1 from $1b_2$ and B_2 from $2a_1$) transitions. The structures E, F, and G are comparatively weak and have term values of 2.24, 1.63, and 0.75 eV, respectively; therefore, they are possibly assigned to the lowest *s*-type (4*s* or 5*s*) and *p*-type (4*p* or 5*p*) Rydberg transitions. In the continuum, two broad bands are observed around 540.80 and 542.69 eV, which are attributable to double excitations or S 3*d*-type shape resonances, because there are no other singly excited valence states than the $1s \rightarrow 3b_1$*, $9a_1$* and $6b_2$* transitions.

References

1) J. Adachi *et al., Chem. Phys. Lett.* **294**, 559 (1998).

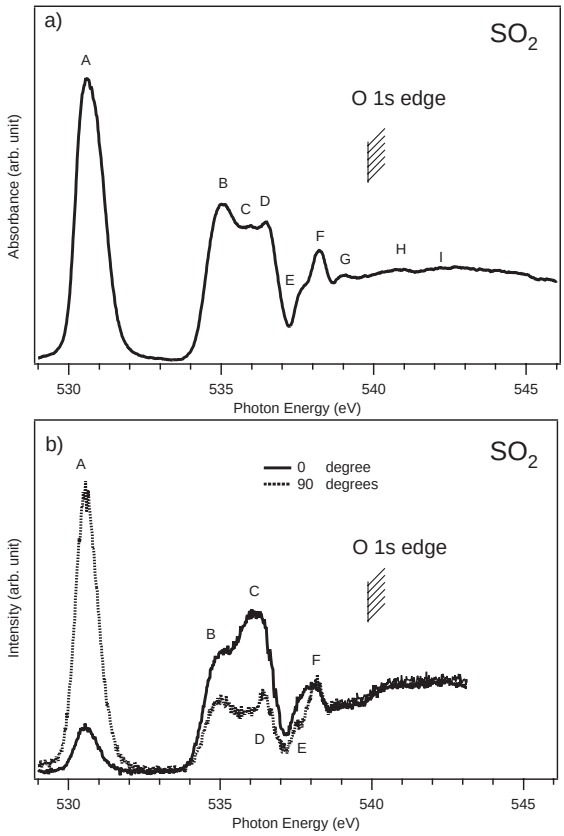

Figure 1. a) Absorption spectrum of SO_2 in the O *K*-edge region. b) Angle-resolved ion yield spectra of SO_2. Dotted and solid lines denote I_{90} and I_0 ion yields, respectively.

VIII-V-6 The Measurement of Absorption Spectra of Trifluoromethyl Sulfur Pentafluoride in VUV Region

GEJO, Tatsuo; SHIGEMASA, Eiji; TAKAHASHI, Kenshi[1]; MATSUMI, Yutaka[1]
([1]Nagoya Univ.)

Global warming or green house effect is one of the major issues for environmental chemistry. Although CO_2, CH_4, and N_2O play a major role on the green house effect in air, some gases with much lower concentrations can contribute to the global warming because of their exceptionally large infrared absorption. For example, SF_6 has 22,200 times larger global warming potential (GWP) over a 100-year time than CO_2 although it is currently present in the atmosphere at only 4 ppt.[1)] Recently Sturges *et al.* detected Trifluoromethyl sulfur pentafluoride (SF_5CF_3), which is chemically close to SF_6, at Antarctic deep consolidated snow (firn).[1)] This Antarctic firn measurement shows that the concentration of SF_5CF_3 have increased from near zero in the late 1960s to about 0.12 ppt in 1999, whose trend matches to recent global warming tendency. They also measured a radiative forcing of SF_5CF_3, which is 0.57 watt per square meter per parts per billion.[1)] This is the largest radiative forcing, on a per molecule basis, of any gas found in the atmosphere up to this date. They also reported stratospheric profiles of SF_5CF_3 and suggested that it is long-lived in the atmosphere (on the order of 1000 years).[1)] If this is true, the irreversible accumulation of this gas may affect the green house effect drastically. In order to access this effect and lifetime of SF_5CF_3 in the stratosphere more precisely, its absorption spectra and cross sections in the VUV region are crucial.

The present photoabsorption measurement of SF_5CF_3 in the VUV region was performed at BL7B in the UVSOR facility. Synchrotron radiation at UVSOR was monochromatized by using a 3-m normal incidence monochromator. The intensity of the photon beam transmitted through a gas cell was monitored by using a silicon photodiode (IRD Inc, AXUV-100). The photoabsorption cross sections were calculated by using the Beer-Lambert expression. The data were checked to ensure there is no line saturation effect.

In the region of interest, two strong peaks in the absorption spectra of SF_5CF_3 were observed: One peak around 107 nm (A) and another one around 130 nm (B). The peak similar to A is also observed in SF_6, whereas the equivalent to the peak B was not observed. Therefore one can suggest that the peak B arises from the transition from the lone pair electron of CF_3.

Based on these data, we will estimate the lifetime of SF_5CF_3 in the stratosphere.

Reference

1) W. T. Sturges *et al.*, *Science* **289**, 613 (2000).

VIII-V-7 Symmetry-Resolved Cl 2*p* Photoabsorption Spectra of Cl_2

SHIGEMASA, Eiji; GEJO, Tatsuo; HATSUI, Takaki; KOSUGI, Nobuhiro

The 2*p* ionization spectra, or photoelectron spectra, show molecular field splittings (MFS) and spin-orbit splittings (SOS). The 2*p* excitation spectra, or photoabsorption spectra, exhibit exchange splittings (EXS) in addition to MFS and SOS. We have already investigated very complicated spectral features due to EXS and SOS in the S 2*p* excitation region of SO_2, CS_2 and OCS, based on angle-resolved photoion spectroscopy (ARPIS) and the Breit-Pauli *ab initio* calculation. In the present work, Cl 2*p* ARPIS spectra of Cl_2 in comparison to HCl are reported. The lowest excited states in these molecules are the Cl 2*p*-π* excitation. There are three 2*p* orbitals, and the Cl 2*p*-σ* excitation involves parallel and perpendicular transitions with respect to the bond direction. We will discuss a propensity rule for the two transition directions by measuring the fragment-ion yields.

The experiments were performed on the newly constructed beamline BL4B at the UVSOR, IMS. ARPIS spectra were measured with two identical ion detectors having retarding grids, which were set at 0° and 90° relative to the electric vector of the light, by scanning the photon energy. The photon-energy resolution was set to about 50 meV for the present experiments. The Cl 2*p* ARPIS spectra of Cl_2 are displayed in Figure 1. The excitation energies and the nature of the structures observed will be discussed with the help of theoretical calculations.

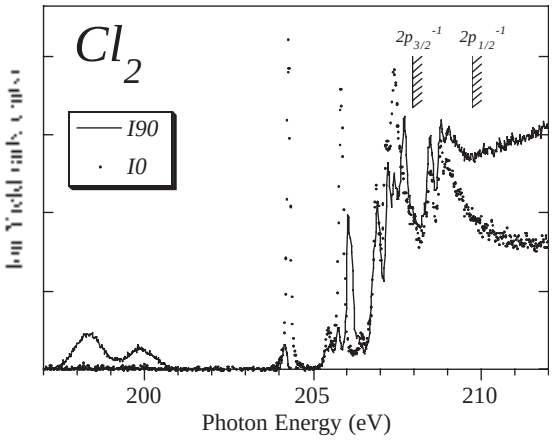

Figure 1. ARPIS spectra in the Cl 2*p* excitation region of Cl_2.

VIII-V-8 Dynamical Angular Correlation in Molecular Auger Decay

GUILLEMIN, Renaud[1]; SHIGEMASA, Eiji; LE GUEN, Karine[1]; CEOLINE, Denis[1]; MIRON, Cataline[1]; LECLERCQ, Nicola[1]; MORIN, Paul[1]; SIMON, Marc[1]
([1]LURE)

[*Phys. Rev. Lett.* **87**, 203001 (2001)]

The first measurements of the angular distribution of Auger electrons from fixed-in-space molecules have been performed in the C *K*-shell ionization region of CO, for both parallel and perpendicular orientation of the molecular axis with respect to the light polarization vector. The ions emitted parallel or perpendicular to the electric vector of the incident radiation determine the possible Σ or Π symmetries in the ionization channels, respectively. The angular distributions obtained for the CO^{2+} $B^1\Sigma$ Auger final state show dramatic spectral

variations, which also depend on the initial ionization channels, Σ or Π. The result strongly suggests the breakdown of the two-step model in which the Auger decay is treated independently of the initial photoionization process.

VIII-V-9 Nondipolar Electron Angular Distributions from Fixed-in-Space Molecules

GUILLEMIN, Renaud[1]; HEMMERS, Oliver[1]; LINDLE, Denis[1]; SHIGEMASA, Eiji; LE GUEN, Karine[2]; CEOLINE, Denis[2]; MIRON, Cataline[2]; LECLERCQ, Nicola[2]; MORIN, Paul[2]; SIMON, Marc[2]; LANGHOFF, Peter[3]
([1]Univ. Nevada; [2]LURE; [3]Univ. California)

[*Phys. Rev. Lett.* **89**, 033002 (2002)]

The first indication of nondipole effects in the azimuthal dependence of photoelectron angular distributions emitted from fixed-in-space molecules is demonstrated in N_2. Comparison of the results with angular distributions observed for randomly oriented molecules and theoretical derivations for the nondipole correction first order in photon momentum suggests that higher orders will be needed to describe distributions measured in the molecular frame.

VIII-V-10 Double and Triple Excitations Near the *K*-Shell Ionization Threshold of N_2 Revealed by Symmetry-Resolved Spectroscopy

SHIGEMASA, Eiji; GEJO, Tatsuo; NAGASONO, Mitsuru; HATSUI, Takaki; KOSUGI, Nobuhiro

[*Phys. Rev. A* **66**, 022508 (2002)]

High-resolution photoion yield spectra of N_2 are measured near the *K*-shell ionization threshold. Previously-unresolved multiple excitations are distinguished in the Σ- and Π-symmetry resolved spectra, which were obtained from the ion yield spectra recorded at 0° and 90° relative to the polarization direction. The three $^1\Pi_u$ and two $^1\Sigma_u^+$ doubly excited states are clearly identified. Furthermore, a weak Π-symmetry feature just at the σ*-shape resonance position (~ 419 eV) is definitely resolved and assigned to the lowest $^1\Pi_u$ triple excitation with the help of quantum chemical calculations.

VIII-V-11 Optical and Magneto-Optical Studies on Electronic Structure of CeSb in the Magnetically Ordered States

KIMURA, Shin-ichi; OKUNO, Mitsuru[1]; IWATA, Hideki[1]; KITAZAWA, Hideaki[2]; KIDO, Giyu[2]; ISHIYAMA, Fumihiko[3]; SAKAI, Osamu[4]
([1]Kobe Univ.; [2]Natl. Inst. Mater. Sci.; [3]Tohoku Univ.; [4]Tokyo Metropolitan Univ.)

[*J. Phys. Soc. Jpn.* **71**, (2002) in press]

The electronic structure of CeSb in the magnetically ordered states is examined by measuring the optical reflectivity, the magnetic linear dichroism and the magnetic circular dichroism spectra at low temperatures under magnetic fields in the infrared region. The optical conductivity spectrum, as well as the reflectivity spectrum changes significantly with the complex magnetic phase diagram, and gives detailed information of electronic structures in the ordered states. The spectra in the ordered states cannot be explained only by the energy band folding due to the appearance of the periodic magnetic structure. By comparing with the calculated optical conductivity spectra, we found that not only the Ce4*f*–Sb5*p* mixing but also the Ce5*d*–Sb5*p* mixing mainly works in the ordered states.

VIII-V-12 Low Energy Electronic Structure of $Ce_{1-x}La_xSb$ (x = 0, 0.1) in the Magnetically Ordered States

KIMURA, Shin-ichi; OKUNO, Mitsuru[1]; IWATA, Hideki[1]; KITAZAWA, Hideaki[2]; KIDO, Giyu[2]
([1]Kobe Univ.; [2]Natl. Res. Inst. Met.)

[*Physica B* **312-313**, 228 (2002)]

The anisotropy of the effect of *pf* mixing on the electronic structure of $Ce_{1-x}La_xSb$ (x = 0, 0.1) in the magnetically ordered states is examined by measuring the magnetic linear dichroism of the optical conductivity spectrum ($\sigma_{//}(\omega)$ for $\boldsymbol{E}//\boldsymbol{B}//[001]$, $\sigma_{\perp}(\omega)$ for $\boldsymbol{E}\perp\boldsymbol{B}//[001]$) in the infrared region at low temperatures under magnetic fields. The $\sigma_{\perp}(\omega)$ spectrum changes significantly with magnetic phase, whereas $\sigma_{//}(\omega)$ changes little. This result indicates that the electronic structure perpendicular to the magnetic field is more strongly modulated by *pf* mixing than that parallel to the field.

VIII-V-13 Temperature Dependence of Low-Energy Optical Conductivity of $Yb_4(As_{1-x}P_x)_3$ (x = 0, 0.05, 0.15)

KIMURA, Shin-ichi; OKUNO, Mitsuru[1]; IWATA, Hideki[1]; AOKI, Hidekazu[2]; OCHIAI, Akira[3]
([1]Kobe Univ.; [2]Max-Planck-Inst., Germany; [3]Tohoku Univ.)

[*J. Phys. Soc. Jpn.* **70**, 2829 (2001)]

To investigate the anomalous transport property and the electronic structure near the Fermi level of Yb_4As_3, we measured the temperature dependence of the reflectivity spectra of $Yb_4(As_{1-x}P_x)_3$ (x = 0, 0.05, 0.15) in the photon energy range of 2 meV–1.5 eV. The optical conductivity spectrum due to carrier absorption (Drude curve) significantly changes with temperature. Above 200 K, the Drude curve with a high effective carrier density (N_{eff}) and a short relaxation time (τ) is commonly observed in all $Yb_4(As_{1-x}P_x)_3$. On the other hand, below 70 K, the Drude curve changes to one with a low N_{eff} and a longτ below 10 meV. At the same temperature, a new peak appears at 15 meV in Yb_4As_3. The Drude curve and the new peak are considered to originate from the bare As 4*p* hole band and the hybridization state between the 4*f* and 5*d* bands on the

Yb^{3+} chain, respectively.

VIII-V-14 Charge Ordering Effect of Electronic Structure of $Yb_4(As_{1-x}Sb_x)_3$

KIMURA, Shin-ichi; NISHI, Tatsuhiko[1]; OKUNO, Mitsuru[1]; IWATA, Hideki[1]; AOKI, Hidekazu[2]; OCHIAI, Akira[3]
([1]Kobe Univ.; [2]Max-Planck-Inst., Germany; [3]Tohoku Univ.)

[*J. Phys. Soc. Jpn.* **71**, 300 (2002)]

The change of the electronic structure near the Fermi level of Yb_4As_3 due to the charge ordering is examined by measuring the temperature dependence of reflectivity spectra of $Yb_4(As_{1-x}Sb_x)_3$ (x = 0, 0.12, 0.24) in the photon energy range of 2 meV–1.5 eV. In the optical conductivity spectra, a peak commonly appears at 0.4 eV below the temperature that is a little higher than the charge ordering temperature. Its intensity increases as the temperature decreases. The peak intensity indicates the ratio of the charge-ordered state for the whole because it originates from the optical transition to the Yb 5*d* band in the charge-ordered state.

VIII-V-15 Temperature-Induced Valence Transition of $EuNi_2(Si_{0.25}Ge_{0.75})_2$ Studied by Eu 4*d*-4*f* Resonant Photoemission and Optical Conductivity

KIMURA, Shin-ichi; OKUNO, Mitsuru[1]; IWATA, Hideki[1]; SAITOH, Tomohiko[2]; OKUDA, Taichi[3]; HARASAWA, Ayumi[3]; KINOSHITA, Toyohiko[3]; MITSUDA, Akihiro[3]; WADA, Hirofumi[4]; SHIGA, Masayuki[4]
([1]Kobe Univ.; [2]Photon Factory; [3]Univ. Tokyo; [4]Kyoto Univ.)

[*J. Phys. Soc. Jpn.* **71**, 255 (2002)]

Eu 4*d*-4*f* resonant photoemission and optical reflectivity measurements of a temperature-induced valence transition material, $EuNi_2(Si_{0.25}Ge_{0.75})_2$, have been performed at several temperatures. The valence transition was observed and the mean valence was evaluated to be 2.37 ± 0.02 and 2.75 ± 0.25 below and above the valence transition temperature, respectively. The mixing between the Ni 3*d* conduction band and the Eu^{3+} 4*f* hole becomes weak as the temperature increases, showing the valence transition from Eu^{3+} to Eu^{2+}.

VIII-V-16 Optical Gap in the Diluted Kondo Semiconductors $Yb_{1-x}Lu_xB_{12}$: Lattice and Single-Site Effects

OKAMURA, Hidekazu[1]; MATSUNAMI, Masaharu[1]; KIMURA, Shin-ichi; NANBA, Takao[1]; IGA, Fumiroshi[2]; TAKABATAKE, Toshiro[2]
([1]Kobe Univ.; [2]Hiroshima Univ.)

[*Physica B* **312-313**, 157 (2002)]

We have studied the evolution of energy gap in the optical conductivity [$\sigma(\omega)$] of $Yb_{1-x}Lu_xB_{12}$ as functions of temperature (T) and non-magnetic Lu substitution (x). YbB_{12} has a well-developed energy gap in $\sigma(\omega)$ below 20 K, with the onset of $\sigma(\omega)$ at ~ 20 meV and a shoulder at ~ 40 meV. With increasing T or x, the energy gap is rapidly filled in, which indicates the importance of coherence among the Yb 4*f* orbitals at different sites. The shoulder, on the other hand, remains nearly unshifted in wide ranges of T (to 70K @) and x (0–1/2), which shows that the characteristic energy for the gap is given by some single-site energy scale of Yb^{3+}. Namely, both lattice and single-site effects play important roles in the gap formation of YbB_{12}.

VIII-V-17 Magneto-Optical Study of the Colossal Magnetoresistance Pyrochlore $Tl_2Mn_2O_7$

OKAMURA, Hidekazu[1]; KORETSUNE, Toshihisa[1]; MATSUNAMI, Masaharu[1]; KIMURA, Shin-ichi; NANBA, Takao[1]; IMAI, H.[2]; SHIMAKAWA, Y.[2]; KUBO, Y.[2]
([1]Kobe Univ.; [2]NEC Corp.)

[*Physica B* **312-313**, 714 (2002)]

Pyrochlore $Tl_2Mn_2O_7$ has been found to exhibit a colossal magneto-resistance (CMR) that is comparable to that for the perovskite manganites such as $La_{1-x}Sr_x$-MnO_3: In order to probe the microscopic electronic structures of $Tl_2Mn_2O_7$; we have measured its optical conductivity $\sigma(\omega)$ in wide ranges of photon energy, temperature (T), and external magnetic field (B). We have observed very strong variations of $\sigma(\omega)$ with T and B near the Curie temperature, where the CMR manifests itself. Analyses on the variations in $\sigma(\omega)$ show that both T- and B-induced evolutions of the electronic structures in $Tl_2Mn_2O_7$ are very similar to each other, and that they are universally related to the development of macroscopic magnetization. We have also observed a pronounced Kerr rotation at the plasma edge of the reflectivity.

VIII-V-18 Influence of Electronic Structure of $CeSbNi_{0.15}$ on its Optical Conductivity

HONG, S. O.[1]; MIN, B. H.[1]; LEE, H. J.[1]; KIMURA, Shin-ichi; JUNG, M. H.[2]; TAKABATAKE, Toshiro[2]; KWON, Y. S.[1]
([1]SungKyunKwan Univ., Korea; [2]Hiroshima Univ.)

[*Physica B* **312-313**, 251 (2002)]

The reflectivity of $CeSbNi_{0.15}$ is measured at several temperatures in the low energy regions. The optical conductivity is obtained from the measured reflectivity. The carrier concentration and the relaxation time are evaluated by the Drude model. It is found that the *pf* mixing collapse takes place in $CeSbNi_{0.15}$ and that the gap formation occurs at 7 K.